Yanbu Journal of Engineering and Science

Volume 20 | Issue 1 Article 4

2023

Modeling and Simulation Study of a Novel Bat Sand Vertical Axial-Wind Turbine

Saeed Almalowi
Taibah University, Saudi Arabia

Majdi T. Amin
Yanbu Industrial College, Saudi Arabia

Follow this and additional works at: https://yjes.researchcommons.org/yjes

The journal in which this article appears is hosted on Digital Commons, an Elsevier platform.

Recommended Citation

Almalowi, Saeed and Amin, Majdi T. (2023), Modeling and Simulation Study of a Novel Bat Sand Vertical Axial-Wind Turbine, *Yanbu Journal of Engineering and Science*: Vol. 20: Iss. 1, 26-31.
DOI: https://doi.org/10.53370/001c.75396
Available at: https://yjes.researchcommons.org/yjes/vol20/iss1/4

This Research Article is brought to you for free and open access by Yanbu Journal of Engineering and Science. It has been accepted for inclusion in Yanbu Journal of Engineering and Science by an authorized editor of Yanbu Journal of Engineering and Science.

Research article

Modelling and Performance Assessment of a Two-Bed Adsorption Chiller at Different Operating Conditions

MAJDI AMIN[1]

[1] Mechanical Engineering Technology, Royal Commission for Jubail and Yanbu

Keywords: Adsorption system, Performance, Methanol, Maxsorb III, Modeling, Low grade heat.

https://doi.org/10.53370/001c.92145

Yanbu Journal of Engineering and Science

Vol. 20, Issue 2, 2023 Submitted: 04 APR 2023 Revised: 05 JUN 2023 Accepted: 20 JUL 2023

The study aims to assess the performance of an adsorption chiller using the Maxsorb III-methanol as an adsorbent pair. A modified transient lumped parameter model was developed to evaluate the dynamic behavior of the system at various operating parameters. Methanol is used as refrigerant as it has a significant latent heat of evaporation, high normal boiling point, low melting point and environmentally friendly. The results showed that the modified transient lumped parameter model can predict well the dynamic behavior of the adsorption chiller under different operating conditions. The system was able to produce about 13.65 kW (227 W kg-1) cooling capacity with a thermal COP of 0.73 at 85 and 30 oC driving source and cooling temperatures respectively. In addition, simulation tests were made to compare the performance of the Maxsorb III-methanol system with the different working pairs at the same physical dimensions of the present system components and operating parameters. At heat source temperatures of 85 oC which can be gained from waste heat or solar energy, the COP of the Maxsorb III-methanol cycle was about 12.0%, 44.0% and 6.6% higher than that of ACF-ethanol, silica-gel-water and activated charcoal/methanol cycles. The Maxsorb III/methanol adsorption cycle can work effectively with low grade heat sources, which can be gained from renewable energy or waste heat sources.

Nomenclature

A	area, m^2	chw	chilled water
C_p	specific heat capacity, J $kg^{-1}k$	cond	condenser
M	Mass, kg	cwa	cooling water in adsorber/desorber
$\dot{m}$	mass flow rate, kg s^{-1}	cwc	cooling water in condenser
p_s	saturated pressure, Pa	des	desorption
U	overall heat transfer coefficient, W $m^{-1}K$	eva	evaporator
ΔH_{st}	isosteric heat of adsorption, J kg^{-1}	in	inlet
Subscripts		out	outlet
Al	aluminum	ref	refrigerant
ac	activated carbon (Methanol III)	w	water
ads	adsorption	**Superscripts**	
Cu	copper heat transfer tube	bed	adsorption/desorption heat exchanger

1. INTRODUCTION

Due to global energy and environmental issues, utilizations of low-grade heat source are becoming one of the main subjects in the energy investigation area nowadays.[1,2] Thermally powered adsorption chillers are becoming one of the possible potentials electrically powered vapor compression cooling systems (VCCSs) in terms of energy saving and environmental protection.[3] They have the advantages of noiseless, low operating costs, low maintenance, eco-friendly refrigerants such as water, ammonia, or methanol. Compared with absorption chillers, do not require pumps (vibrationless), less sensitive to shocks and do not contain any hazardous materials.[4,5]

A widespread application of adsorption chillers in practice is limited by its rather low coefficient of performance

(COP) values and cooling capacity, due to the heat losses in the used heat exchangers.[6] However, these problems can be dominated by providing new system design, configurations, and new working pairs.[7] In addition, utilizes new heat exchangers adsorbent beds.[8,9] In recent years there has been increased attention to applying low-grade heat sources including solar and waste heat as a driving source for cooling applications. The need for cooling and the availability of sunshine both normally attain maximum levels at the same time. Waste heat can be gained freely from factories, power stations, diesel engines, and chemical plants. Therefore, using these sources to drive adsorption system is a good idea due to mainly both sources are clean, available, and green source of energy.[10]

Many investigations have been focused on improving the performance of adsorption chillers with different methods. Some experimental investigations on the performance of adsorption chillers have been conducted for different system designs can be found in the open literature such as.[11, 12] Most of the investigations on the performance of adsorption chillers have been conducted by the development of mathematical models. Different simulation models have been presented in the open literature. The main differences among these models are in the simplifying assumptions, components design and application of the modelled system. Most researchers use zero-dimensional models where the equilibrium temperature and mass content of the refrigerant depend only on the time variable.[13-16] Extensive studies are also conducted on the characteristics of new adsorbent/adsorbate pairs.[17-23] The most used adsorbent in the literature is silica gel, zeolites and activated carbons. Activated carbons are the most effective adsorbent due to large surface area and porosity.[24] The mean surface area of activated carbon, silica gel, and zeolite is about 200-1200, 300- 850 and 600-700 m^2g^{-1} respectively, while the particle porosity is 40-85, 47-71 and 20-50 %, respectively.[25,26]

The widely used adsorbate in cooling and heat pump systems are methanol, ammonia, and water which have a comparatively large latent heat of vaporization values of about 1100, 1368 and 2200 $kJkg^{-1}$, respectively.[27] The large values of latent heat of evaporation, the availability, and the safety use of the water make it the ideal refrigerant. However, the low vapor pressure and freezing point of the water limit its application in the cooling systems, cannot be used for applications below 0 C. On the other hand, ammonia is toxic and corrosive but can be used for applications with temperatures below 0 C. The low melting point of methanol (-93.9 ^oC) permits us to generate cooling below 0 C temperatures in applications such ice makers, air conditioning, and refrigeration systems. Due to its small latent heat of evaporation, dissociation problems can be encountered at higher temperatures above 120 ^oC.[26] In addition, the high boiling point (64.7 ^oC) presents an important safety factor when there is a leakage. Therefore, higher COP of adsorption cycle with methanol can be provided due to its significant thermal properties.[28]

Activated carbon is one of the most widely used adsorbents in adsorption chillers due to its properties that include high surface area and porosity. Different types of activated carbon with different properties have been studied and proposed in previous literature as adsorbents in the adsorption chillers. Activated carbon with different types with methanol as working pairs have also been investigated for use in solar powered adsorption ice maker and adsorption cooling system. Activated carbon-methanol is favorable adsorbent pairs used in adsorption systems with large adsorption quantity of around 1800-2000 $kJkg^{-1}$ and low desorption temperature of 100 °C.[29,30]

Table 1 summarizes the experimental and theoretical studies that employ the different types of activated carbon-methanol as working pairs in various applications. As can be seen that, activated carbon-methanol pairs-based adsorption system is used widely for freezing applications with heat source temperatures below 100 ^oC.

Maxsorb III is a type of activated carbon. Compared with other activated carbon materials, Maxsorb III has various physical and interesting properties such as large surface area and great adsorption capacity.[42] This makes it preferable than activated carbons in adsorption applications.[43] As shown in the literature, activated carbon-methanol is favorable adsorbent pairs. Different investigations are conducted on the utilization of various types of activated carbon with methanol as working pairs. The utilization of Maxsorb III with methanol as working pairs in adsorption chiller has not been investigated yet. From this above perspective, the present study aims to investigate the performance of Maxsorb III-methanol adsorption chiller at different operating conditions. A modified transient lumped parameter model was developed to evaluate the dynamic behavior of the system under different operating conditions. To our knowledge, the performance of adsorption chillers employing Maxsorb III-methanol as a working pair has not been investigated yet.

2. DESCRIPTION OF THE TWO-BED MAXSORB III/METHANOL ADSORPTION CHILLER

Figure 1 presents the schematic of a proposed adsorption chiller. The system contains mainly different heat exchangers (namely, condenser, evaporator, two adsorber/desorber) and valves.

The cycle contains mainly two modes (Mode I and II) run alternately as shown in Figure (1) and (2) respectively. In the first mode (I), the Bed (A) is considered as desorber and Bed (B) as adsorber. In this mode, both valves (V_2) and (V_4) are opened. On the other hand, valves (V_1) and (V_3) are closed. The adsorbent Bed (B) is cooled down by the flow of water coming from the cooling water tank (Q_{ads}). This makes the refrigerant vapor (methanol) flow from the evaporator adsorbed by the Maxsorb III in the Bed (B). At the same time, Bed (A) is heated by Q_{des} provided by the available waste heat and this causes the methanol in it to be desorbed. The methanol then flows to the condenser via valve (V_2) to be condensed. The methanol vapor in the condenser element is cooled by flow water $\dot{Q}_{cond}$. The condensed methanol liquid returns to the evaporator element through the expansion valve and is adsorbed by adsorbent Bed (B) until the methanol liquid is saturated in the adsorber. After a time

Table 1. Summary of activated carbon-methanol pairs for adsorption cooling systems.

Ref.	Adsorbent - adsorbate pair	Application	System COP	System characteristics
31	Activated carbon - methanol	Combined cooling, heating, and power	0.12	1000 kW combined cooling
32	ADC-2P activated carbon-methanol	a Tri–Generation cooling system	0.34-0.98	10 kW cooling capacity
33	activated carbon-methanol	Cooling	0.169	32 kW cooling capacity
34	Activated carbon (AC35) - methanol	Solar powered ice making	0.11	Two bed system Cooling produced/day = 266.8 kj/m2
35	Solidified activated carbon - methanol	Ice making driven by waste heat	0.085 - 0.18	Two and three bed system
36	Activated carbon (AC35) - methanol	Solar powered ice making	0.19	Ice produced= 11.5 kg/ day/m^2
37	Activated carbon - methanol pair	Solar powered ice making	0.124-0.155	Two bed system Ice produced = 7 - 10 kg/ day/m^2
38	Activated carbon (charcoal) - methanol	Solar powered ice making	0.1 - 0.12	Ice produced = 4 - 5 kg/ day/m^2
39	Active carbon (Charcoal) - methanol	Solar powered ice making	0.02	Two bed system
40	Active carbon (AC35) - methanol	Cooling system	0.5	Two bed system
41	Activated Carbon (AC35) - methanol	Solar powered making	0.12	Ice produced = 30 - 35 kg/ day/m^2

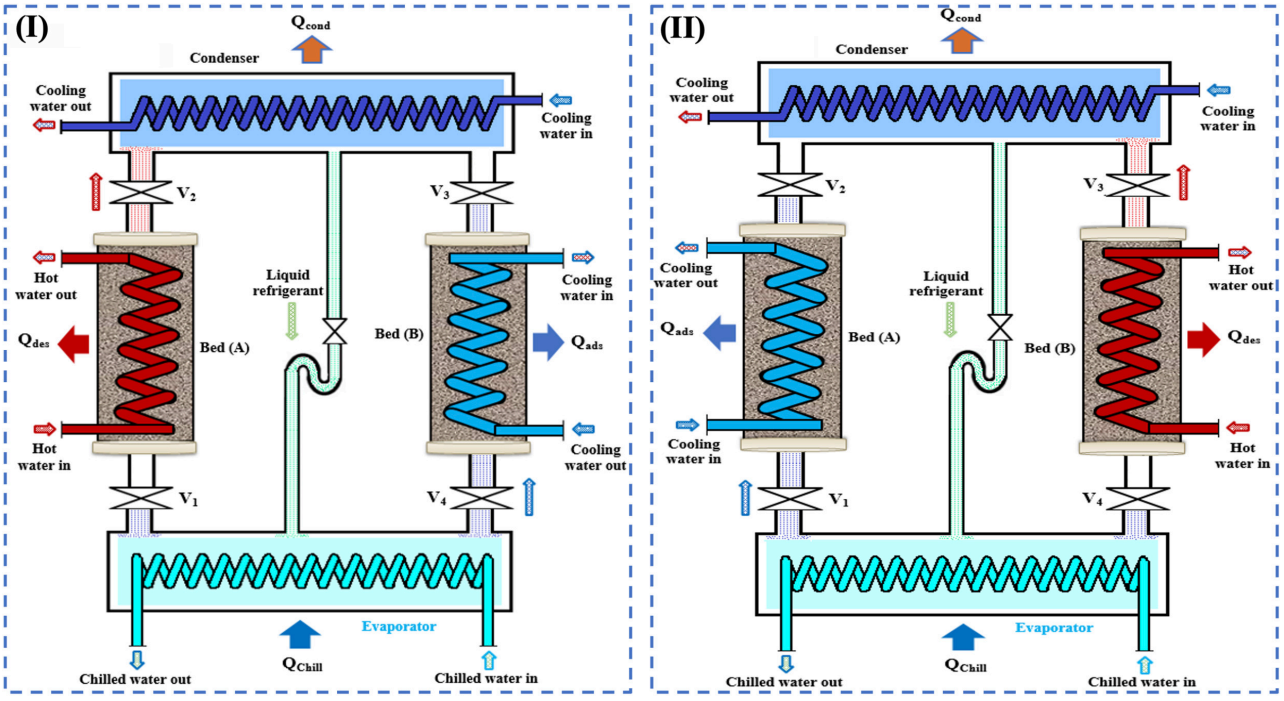

Fig. 1. Schematic diagram of two-bed Maxsorb III-methanol adsorption chiller during mode (I) and mode (II)

period, the cycle is continued by switching the operation from mode (I) to mode (II). Again, after running in mode (II) for a period, the cycle returns to mode (I).

3. MATHEMATICAL MODEL

The developed mathematical model of the adsorption cooling system consists of the main used assumptions, energy conservation equations, and mass balance of the methanol.

3.1. MAIN ASSUMPTIONS

1. The pressure and temperature distributions and the refrigerant vapor adsorbed are uniform throughout the heat exchanger beds.
2. The properties of the adsorbate vapor and heat exchangers are constant.
3. The heat exchanger beds are well-insulated.
4. Ideal gas behavior has been considered.

3.2. ADSORPTION ISOTHERM AND KINETICS

The adsorption equilibrium for Maxsorb III/methanol vapor is given by the Dubinin Raduskevich (D-R) equation:

$$W = \mathrm{W}_0 \exp\left\{-\mathrm{D}\left(\mathrm{T}\ln\left(\frac{P_s}{P}\right)\right)^n\right\} \tag{1}$$

Based on our previous work,[19] the numerical values of W_0 and D are evaluated practically 1.24 kg methanol/kg Maxsorb III and 4.022×10^{-6} K^{-2} respectively.

Modeling the rate of adsorption/desorption of Maxsorb III/methanol by the linear driving force equation. The present author investigated previously the kinetics of Maxsorb III/methanol pair where the different coefficients such as diffusion time constant (D_s/R_p^2) and $\mathrm{k_s a_v}$ are obtained by tracking the experimental vapor uptake.[44] The Non-equilibrium adsorption rate of Maxsorb III/methanol is given by:

$$\frac{\partial \mathrm{w}}{\partial \mathrm{t}} = \mathrm{k_s a_v}(\mathrm{W}-\omega) \tag{2}$$

$$\mathrm{k_s a_v} = \mathrm{F}_0\frac{\mathrm{D_s}}{\mathrm{R_p^2}} \tag{3}$$

In this equation, $\mathrm{R_p}$ is the radius of Maxsorb III particles (3.6×10^{-5} m). Considering the spherical shape of Maxsorb III. The surface diffusivity ($\mathrm{D_s}$) given by:

$$\mathrm{D_s} = \mathrm{D_{s0}}\exp\left(-\frac{\mathrm{E_a}}{\mathrm{RT}}\right) \tag{4}$$

where, R is universal ideal gas constant and T is the temperature. The pre-exponential $\mathrm{D_{so}}$ and activation energy $\mathrm{E_a}$ are 6.34×10^{-11} $\mathrm{m^2 s^{-1}}$ and 370 kJ $\mathrm{kg^{-1}}$, respectively.[44] The extracted data were reconfirmed by applied non-isothermal adsorption mathematical model.

Isosteric heat of adsorption is one of required thermodynamic parameter for designing of an adsorption chiller. The heat of adsorption of Maxsorb III/methanol is determined practically[44]:

$$\Delta \mathrm{h_{st}} = \mathrm{h_{fg}} + \mathrm{E}\left[\left\{\ln\left(\frac{\mathrm{W_0}}{\mathrm{W}}\right)\right\}^{\frac{1}{\mathrm{n}}} + \mathrm{A}\left(\frac{\mathrm{T}}{\mathrm{T_c}}\right)^{\mathrm{B}}\right] \tag{5}$$

where, the adsorption characteristics E=138 $\mathrm{kJkg^{-1}}$, the maximum uptake $\mathrm{W_0}$=1.24 $\mathrm{kgkg^{-1}}$, $\mathrm{T_c}$= 489.15 k and n=2.

3.3. ENERGY CONSERVATION EQUATIONS

The energy conservation equations of the adsorption cooling system consist of the energy balance of the different system components including adsorber/desorber, condenser, and evaporator.

3.3.1. ADSORBER AND DESORBER

Based on the assumptions mentioned previously in the subsection (3.1), energy balance for adsorber/desorber beds given by:

$$\begin{aligned}&\left[\mathrm{M_{ac}}\left(\mathrm{C_{p,ac}}+\mathrm{C_{p,ref}}\omega_\mathrm{i}\right)\right.\\&\left.\quad+\left(\mathrm{M_{Cu,bed}C_{p,cu}}+\mathrm{M_{Al,finbed}C_{p,Al}}\right)\right]\frac{\mathrm{dT_i^{bed}}}{\mathrm{dt}}\\&=\varphi\Delta\mathrm{h_{st}M_{ac}}\frac{\mathrm{d}\omega_\mathrm{i}^{\mathrm{bed}}}{\mathrm{dt}}+\left(\dot{\mathrm{m}}_\mathrm{w}\mathrm{C_{p,w}}\right)_\mathrm{j}\left(\mathrm{T_{in}}-\mathrm{T_{out}}\right)_\mathrm{j}\\&\quad+\mathrm{M_{ac}C_{p,ref}}\left(\mathrm{T_s}-\mathrm{T_i}\right)\frac{\mathrm{d}\omega_\mathrm{i}^{\mathrm{bed}}}{\mathrm{dt}}\end{aligned} \tag{6}$$

The left-hand side of Eq. (6) shows the internal energy during adsorption and desorption process due to the mass of adsorbent/adsorbate beds content and adsorber/desorber heat exchangers (including the pipes and fins).

Considering the heat transfer from the cooling water to the adsorber bed and the heat transfer from the heating water to the desorber bed. The outlet temperature of the cooling/heating water given by the log mean temperature difference approach, since the temperature differences is small:

$$\mathrm{T_{j,out}} = \mathrm{T_i^{bed}} + \left(\mathrm{T_{j,in}}-\mathrm{T_i^{bed}}\right)\exp\left(\frac{-(\mathrm{UA})_\mathrm{i}^{\mathrm{bed}}}{\left(\dot{\mathrm{m}}\mathrm{C_p}\right)_\mathrm{j}}\right) \tag{7}$$

3.3.2. CONDENSER

The valve between the condenser and desorber element is opened through the desorption process, so that the adsorbate (methanol) from the desorber bed is condensed in the condenser.

$$\begin{aligned}&\left[\mathrm{M_{ref,cond}C_{p,ref}}+\mathrm{M_{cond}C_{p,Cu}}\right]\frac{\mathrm{dT_{cond}}}{\mathrm{dt}}\\&=-\varphi\mathrm{h_{fg}M_{ac}}\frac{\mathrm{d}\omega_{\mathrm{des}}}{\mathrm{dt}}+\left(\dot{\mathrm{m}}\mathrm{C_p}\right)_{\mathrm{cw,cond}}\left(\mathrm{T_{in}}-\mathrm{T_{out}}\right)_{\mathrm{cw}}\\&\quad+\varphi\mathrm{M_{ac}C_{p,ref}}\left(\mathrm{T_{cond}}-\mathrm{T_{des}}\right)\frac{\mathrm{d}\omega_{\mathrm{des}}}{\mathrm{dt}}\end{aligned} \tag{8}$$

The outlet temperature of the cooling water from the condenser given by:

$$\begin{aligned}\mathrm{T_{cwc,out}} = \mathrm{T_{cond}}&+\left(\mathrm{T_{cwc,in}}-\mathrm{T_{cond}}\right)\\&\times\exp\left(\frac{-(\mathrm{UA})_{\mathrm{cond}}}{\left(\dot{\mathrm{m}}\mathrm{C_p}\right)_{\mathrm{w,cond}}}\right)\end{aligned} \tag{9}$$

3.3.3. EVAPORATOR

The energy balance here is dominated by the heat and mass interactions between the adsorber and the evaporator as well as the heat emitted from the condenser via the expansion valve as the follows:

$$\begin{aligned}&\left[\mathrm{M_{ref,eva}C_{p,rf}}+\mathrm{M_{eva}C_{p,Cu}}\right]\frac{\mathrm{dT_{eva}}}{\mathrm{dt}}\\&=-\varphi\mathrm{h_{fg}M_{ac}}\frac{\mathrm{d}\omega_{\mathrm{ads}}}{\mathrm{dt}}+\left(\dot{\mathrm{m}}\mathrm{C_p}\right)_{\mathrm{chw}}\left(\mathrm{T_{in}}-\mathrm{T_{out}}\right)_{\mathrm{chw}}\\&\quad+\varphi\mathrm{M_{ac}C_{p,ref}}\left(\mathrm{T_{eva}}-\mathrm{T_{cond}}\right)\frac{\mathrm{d}\omega_{\mathrm{des}}}{\mathrm{dt}}\end{aligned} \tag{10}$$

Using the LMTD approach, the outlet chilled temperature given by:

$$\begin{aligned}\mathrm{T_{chw,out}} = \mathrm{T_{eva}}&+\left(\mathrm{T_{chw,in}}-\mathrm{T_{eva}}\right)\\&\times\exp\left(\frac{-(\mathrm{UA})_{\mathrm{eva}}}{\left(\dot{\mathrm{m}}\mathrm{C_p}\right)_{\mathrm{w,eva}}}\right)\end{aligned} \tag{11}$$

Table 2. Design parameters of the adsorption cooling system used in the simulation.

Symbols	Value	Unit
$(UA)_{bed}$	1200×2.46	WK^{-1}
$(UA)_{cond}$	4115.23×3.73	WK^{-1}
$(UA)_{evap}$	2557.54×1.91	WK^{-1}
$M_{Cu,bed}$	51.2	kg
$M_{Al,finbed}$	64.04	kg
M_{cond}	24.28	kg
M_{evap}	12.4	kg
M_{ac}	60	kg
$C_{p,Al}$	0.905	$kJKg^{-1}k$
$C_{p,Cu}$	0.386	$kJKg^{-1}k$
$C_{p,w}$	1.186	$kJKg^{-1}k$
$C_{p,ac}$	0.650	$kJKg^{-1}k$

3.4. MASS BALANCE OF THE METHANOL

The mass balance of methanol in the evaporator element can be written:

$$\frac{dM_{ref,eva}}{dt} = -M_{ac}\left(\frac{d\omega_{des}}{dt} + \frac{d\omega_{ads}}{dt}\right) \quad (12)$$

3.5. MEASUREMENT OF SYSTEM PERFORMANCE

Performance of adsorption chiller given by:

$$SCP = \frac{(\dot{m}C_p)_{chw}\int_0^{tcycle}(T_{chw,in} - T_{chw,out})dt}{M_{ac}t_{cycle}} \quad (13)$$

$$COP = \frac{(\dot{m}C_p)_{chw}\int_0^{tcycle}(T_{chw,in} - T_{chw,out})dt}{(\dot{m}C_p)_{des}\int_0^{tcycle}(T_{hw,in} - T_{hw,out})dt} \quad (14)$$

Tables 2 and 3 show the design parameters of the system and operating conditions of the working fluids used in the modeling, respectively.

4. RESULTS AND DISCUSSION

To investigate the performance of the proposed Maxsorb III/methanol adsorption chiller, cyclic simulation with the developed dynamic model is conducted. The main objective of the present work is to apply a proposed modified transient lumped parameter model to evaluate the dynamic behavior of the system at various operating parameters. Low grade heat source is used as a driving source between 50 and 95°C at ambient temperate coolant.

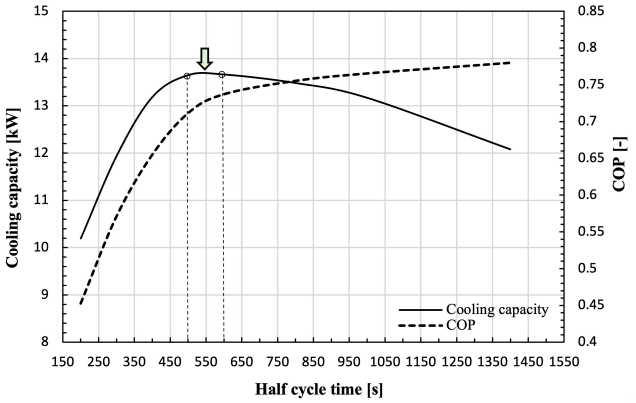

Fig. 2. Half cycle time vs. cooling capacity and system COP for Maxsorb III/Methanol two-bed system.

4.1. HALF CYCLE AND SWITCHING TIME AFFECT THE SYSTEM PERFORMANCE.

Figure 2 shows the simulation data of the effect of the changing half cycle (adsorption/desorption time on cooling ef-fect and system COP at the working conditions listed in Table (3). As shown from the figure, at half cycle time of 550 s or between 500 and 600 s, the cooling capacity is op-timized. At the half-cycle time below 500 s there is not suf-ficient time for adsorption or desorption process to occur satisfactorily so that these processes are not fully accom-plished and the cooling capacity decreases. At the half cycle are longer than 600 s, the cooling effect minimizes gradually with time due to the less intense of adsorption. The system COP growing with the cycle time. This is because of the lower consumption of driving heat with longer duration cycle time.

Figure 3 shows the effect of switching time variation on the cooling effect and system COP of the Maxsorb III/Methanol adsorption chiller. The cooling effect reaches a higher value at switching time of 35 s or between 30 and 40 s. The switching time is shorter than 30 s or more than 40 s; the cooling capacities decrease abruptly. On the other hand,

Table 3. Heat transfer fluids inlet parameters for the adsorption cooling system

Parameter	Symbols	Value	Unit
Heat source temperature	$T_{hw,in}$	85	°c
Adsorber inlet temperature	$T_{cwa,in}$	30	°c
Condenser cooling water inlet temperature	$T_{cwc,in}$	30	°c
Chilled water inlet temperature	$T_{chw,in}$	14	°c
Heat source mass flow rate	$\dot{m}_{mhot}$	1.5	Kgs^{-1}
Adsorber cooling water mass flow rate	$\dot{m}_{cwa}$	1.5	Kgs^{-1}
Condenser cooling water mass flow rate	$\dot{m}_{cwc}$	1.5	Kgs^{-1}
Chilled water mass flow rate	$\dot{m}_{ch}$	0.7	Kgs^{-1}

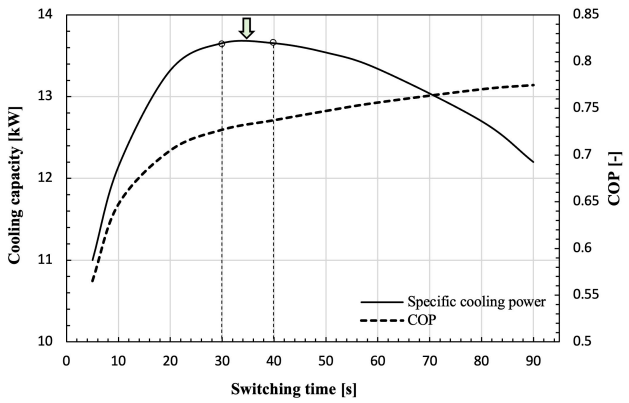

Fig. 3. Switching time vs. cooling effect and system COP for Maxsorb III/Methanol two-bed system

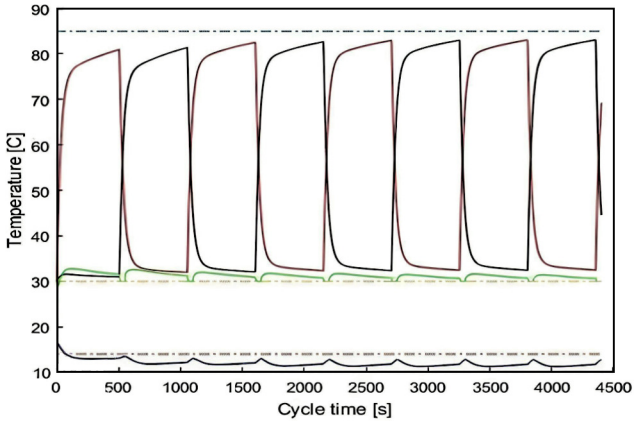

Fig. 4. Temperature profile for different system components of Maxsorb III/methanol two-bed systems

the COP rises rapidly in the range between 0 and 20 s. After this value that the enhancement in system COP is only gradual.

4.2. TEMPERATURE PROFILES OF DIFFERENT SYSTEM COMPONENTS

As shown in the last section, the half cycle time is set as 550 s and switching time of 35 s. The temperature profiles of the components (heat exchangers) of the proposed adsorption chiller with inlet heat transfer fluid temperatures are shown in Figure 4 at the rated values of Table (3). As can be seen from the figure, after about 2 adsorption/desorption cycle times (1176 s), the simulation results of Maxsorb III/methanol two-bed system reaches the cyclical steady state operation. This is because the hot water outlet temperatures from the desorber approach the inlet temperature value of 85°C as mentioned before in simulation procedures of the model program. It should be noted that during the first 550 s one of the beds acts as desorber and at the same time the second bed acts as adsorber.

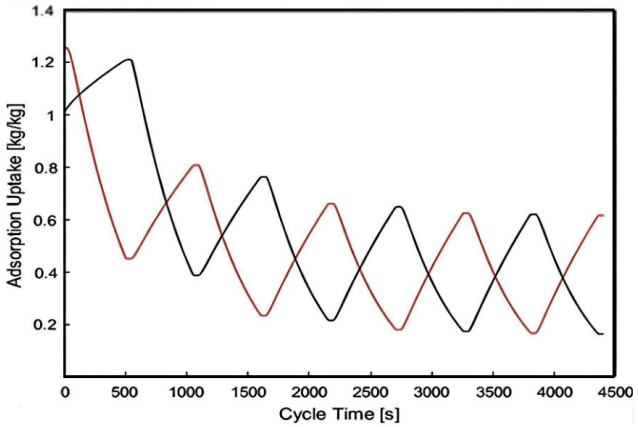

Fig. 5. Time variation of methanol refrigerant content in two beds

4.3. THE TIME VARIATION OF REFRIGERANT CONTENT

The methanol (refrigerant) content in the beds at the standard operating conditions is presented in Figure 5. In the steady stat operation (after 1176 s)the adsorbent in bed A is in adsorption process (Mode II). The refrigeran content of bed A increases to about 0.62 kgkg-1. At the same time,bed B is in desorption process, the refrigerant content in the bed minimizes to around 0.2 kgkg-1.

4.4. EFFECT OF OPERATING PARAMETERS ON THE SYSTEM PERFORMANCE

To investigate the effect of operating parameters on the system performance, the operating parameters shown previously in Table 3 are changed. Figure 6 presents the stim- l ated system performance in terms of system SCP and system COP versus the heat source temperature along with fixed other parameters. It is found that, increase the hot water inlet temperature results in a high SCP and COP. At the higher inlet temperatures, the refrigerant is desorbed rapidly causing more methanol to be adsorbed during the next cycle resulting in elevated performance. It happens since the needed for heat input becomes significantly high when the temperature between heat source and heat sink is large. The specific cooling power rises linearly with the heat source temperature from 9.11 to 265.5 W kg^{-1} as the inlet temperature increased from 50 to 95 ^{o}C. It is notes from Figure 6 that the proposed system can work with low temperatures below 50 ^{o}C which is very small compared to the ice maker application, which is higher than 75 °C.

The system COP also increase with raising hot water temperatures. Increasing the generation temperatures is very effective below 75 ^{o}C, above that the increase in the system COP is only marginal. The heat consumed to desorb methanol from Maxsorb III becomes close to the cooling capacity. The decrease in COP between 75 and 95 ^{o}C is due to the raise in the heat losses at elevated temperatures. It should be noted also from Figure 6 at generation tempera -ture of 85 ^{o}C, the adsorption system is capable of generating capacity of 13.65 kW at COP= 0.73 and average chilled water temperature of 8.8 ^{o}C during the steady state condi-

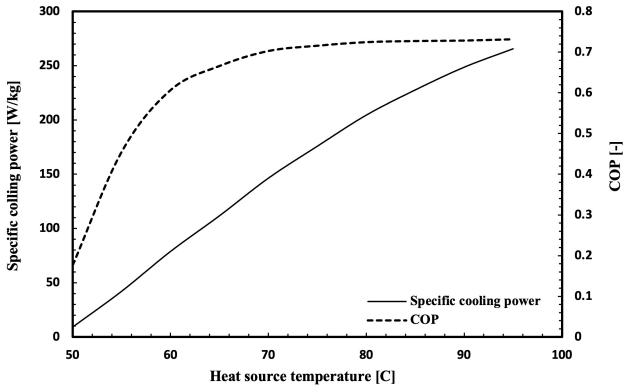

Fig. 6. Influence of driving heat source temperature on SCP and COP

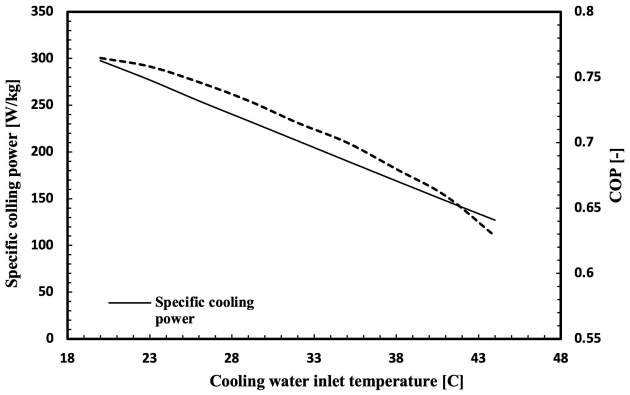

Fig. 8. Variation of cooling water inlet temperature vs. system SCP and COP

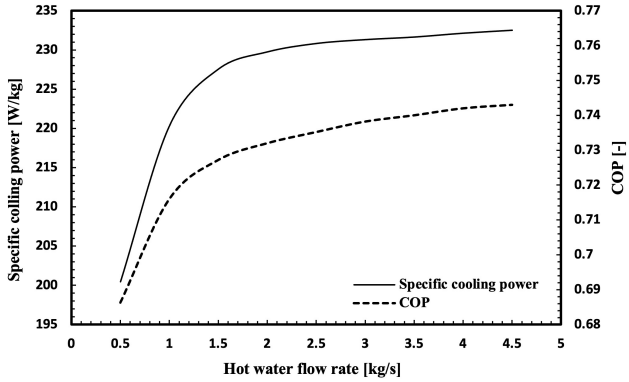

Fig. 7. Variation of hot water flow rate vs system SCP and COP.

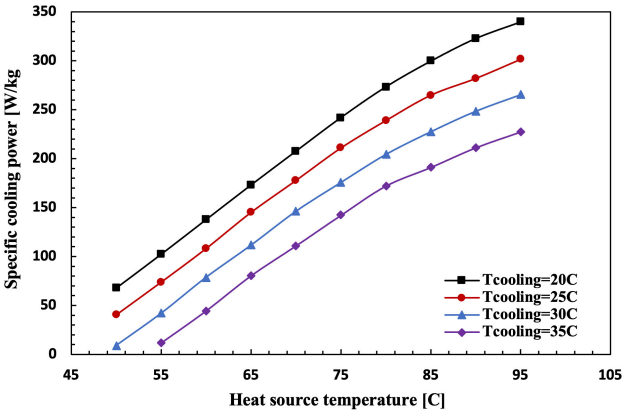

Fig. 9. Variation of hot water inlet temperature vs. system SCP at different inlet cooling water temperatures.

tions. Therefore, the developed Maxsorb III/methanol adsorption chiller is attractive for refrigeration and air conditioning applications using low grade heat source which can be acquired from solar energy.

Figure 7 Displays the effect of the mass flow rate of the heat source water on the SCP and COP of the Maxsorb II/methanol adsorption system. The hot water flow rates are chosen from Table 4, while the other operating parameters were constants as listed in Table 3. As shown increasing hot water flow rates increase both the SCP and COP. However, it can be noticed that both SCP and system COP increase sharply in the range below 2 kgs^{-1}, above that range there is no significant change.

Figure 8 shows variations of cooling watertemperature o n the system SCP and system COP of the system with fixed other operating parameters as shown in Table 3. The simulated SCP and system COP values rise linearly with lower cooling water temperatures, in the entire range studied. This is due to methanol adsorbed by the Maxsorb II raises with minimum adsorbent temperatures. High values of cooling water temperature results in a high temperature in the adsorbent bed. For energy saving, it is recommended to utilize the condenser and bed cooling water at room temperature. Therefore, the present proposed adsorption cooling system is appropriate to utilize cooling water at room temperature including if the inlet temperature may increase up to 30 ^{o}C.

presents the variations of hot water inlet temperatures vs the specific cooling capacity at different cooling water inlet temperatures. The chilled water temperatures and water flow rates are constant as shown in Table 3.

It can be observed, as the hot water inlet temperature increase and/or the cooling water inlet temperature decrease the SCP will increase linearly. As mentioned before, this is since higher desorption temperatures and/or minimum adsorption temperatures result in high mass of methanol adsorbed and desorbed through each cycle. For cooling water inlet temperatures of 20, 25, 30 and 35 ^{o}C, the adsorption chiller can produce 359, 317, 273 and 229 Wkg^{-1}, respectively. A good stable cooling effect can be obtained by the present system.

Finally, Figure 10 demonstrates the variation of chilled water inlet temperature on the system SCP and system COP of the proposed system at constant other operating parameters as listed in Table 3. It is shown that, both specific cooling power and system COP of the system increase linearly with the chilled water inlet temperatures. A 10°C raise in the temperature of the chilled water results in a 7% en-

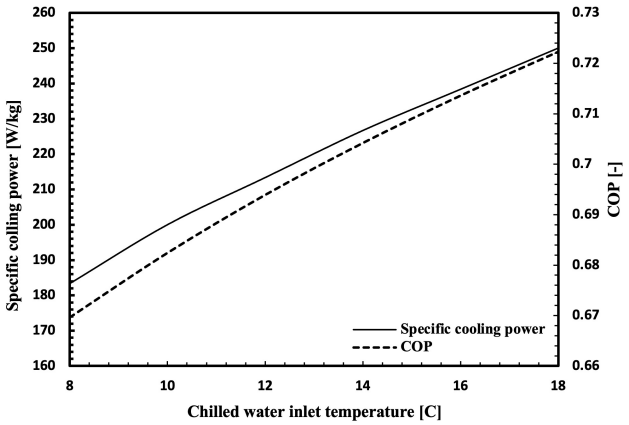

Fig. 10. Variations of chilled water inlet temperature vs the system SCP and system COP.

hancement in the system COP and around 36% increase system SCP at the operating conditions. Therefore, a minor effect can be obtained due to the variation of chilled water inlet temperature.

5. MAXSORB III/METHANOL SYSTEM PERFORMANCE COMPARISON

To evaluate and compare the performance of the proposed Maxsorb III/methanol adsorption system, simulation tests were performed with the same model but at different adsorbent pairs (different equilibrium uptake and adsorption rate equations). The comparison was based on the same dimensions of the system parameters that are shown in Table 2 and the same operating parameters shown in Table 3. The working pairs considered in the study were ACF-ethanol,[20] activated charcoal-methanol[19] and silica gel-water.[45] The maximum uptake of Maxsorb III-methanol, ACF (A20)-ethanol, activated charcoal-methanol and silica gel-water pairs are 1.24, 0.797, 0.705 and 0.3 kg/kg, respectively. Figure 11 (a, b) show the effect of heat source temperature s on the cooling capacity and system COP of the system fo r the dif-ferent working pairs.

As shown from Figure 11,the simulation data showed that both the cooling effect and system COP of the present Maxsorb III-methanol adsorption system are higher than of those of the other pairs. At generation temperatures of 85 oC which could be obtained from solar energy or waste heat, the COP of Maxsorb III-methanol cycle is about 12.0% higher than that of ACF-ethanol cycle, 44.0 % higher than that of silica-gel-water and nearly the same values of about 6.6% improvement over Activated charcoal/methanol cycle. The higher COP of the methanol cycle than ethanol cycle can be related due to the significant enthalpy of vaporization of methanol as mentioned previously, for that methanol always applied for cooling by solar energy. Highly porous Maxsorb III possesses high surface area and pore volume, exhibits fast kinetics as compared with ACF, activated charcoal and silica-gel adsorbent. Methanol has been selected as a refrigerant for its superior thermodynamics properties and is widely used in solar ice making applications.

6. CONCLUSIONS

Thermally driven adsorption chiller considered one of the possible alternatives to traditional vapor compression cooling systems. However, these cycles have low coefficient of performance (COP). These problems can be dominated by providing new system design, configurations, and new working pairs. The utilization of Maxsorb III with methanol as working pairs in adsorption chiller has not been investigated yet. Therefore, this study aims to investigate the performance of two-bed adsorption chiller employed Maxsorb III-methanol as working pairs. The system will be driven by lo grade heat source between 50 and 95 ^{o}C. A modified transient lumped parameter model was developed to evaluate the dynamic behavior of the system under different operating conditions. Performance of the Maxsorb III-methanol system was compared with different systems found in the literature working with various pairs at the same physical dimensions of the present system components and operating parameters. Some conclusion points can be drawn as follows:

- The developed modified transient lumped parameter model can predict well the behavior of the adsorption cycle under various operating conditions.
- The system can produce about 3.65 kW (227 W kg^{-1}) cooling effect with system COP of 0.73 at driving source temperature of 85 ^{o}C, which could be obtained from low grade heat source.
- The Maxsorb III-methanol cycle has a better COP than cycles working with ACF-ethanol, silica-gel-water and activated charcoal/methanol-based by 12.0%, 44.0% and 6.6% respectively.
- The high COP presents the considerable advantage of the proposed working pair-based system.
- Maxsorb III/methanol adsorption cycle can work effectively with low grade heat sources, which can be gained from renewable energy or waste heat sources.

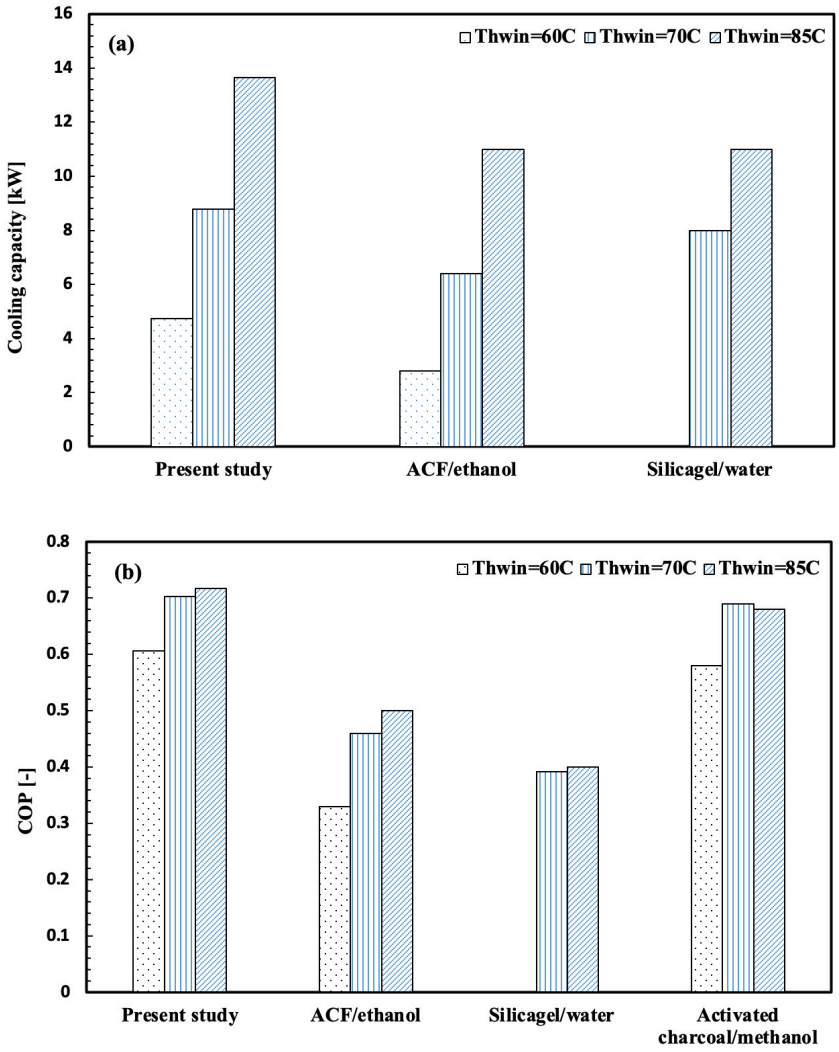

Fig. 11. Variations of generation temperatures vs. a) cooling effect and b) system COP of the system at different working pairs

This is an open-access article distributed under the terms of the Creative Commons Attribution 4.0 International License (CCBY-4.0). View this license's legal deed at http://creativecommons.org/licenses/by/4.0 and legal code at http://creativecommons.org/licenses/by/4.0/legalcode for more information.

REFERENCES

1. Harby K, Al-Amri F. An investigation of energy savings in a split air-conditioner using commercial cooling pads with different thicknesses and wide range of climatic conditions. *Energy*. 2019;182:321-336. doi:10.1016/j.energy.2019.06.031

2. Harby K, Doaa RG, Nader SK, Mohamed SS. Performance improvement of vapor compression cooling systems using evaporative condenser: An overview. *Renew Sust Energ Rev*. 2016;58:347-360. doi:10.1016/j.rser.2015.12.313

3. Hamdy M, Askalany AA, Harby K, Koraa N. An overview on adsorption cooling systems powered by waste heat from internal combustion engine. *Renew Sust Energ Rev*. 2015;51:1223-1234. doi:10.1016/j.rser.2015.07.056

4. Harby K, Almohammadi KM. Study of a new solar-powered combined absorption-adsorption cooling system (ABADS). *Arab J Sci Eng*. 2021;46(3):2929-2945. doi:10.1007/s13369-020-05288-7

5. Harby K, Ali ES, Almohammadi KM. A novel combined reverse osmosis and hybrid absorption desalination-cooling system to increase overall water recovery and energy efficiency. *Journal of Cleaner Production*. 2021;287:125014. doi:10.1016/j.jclepro.2020.125014

6. Almohammadi KM, Harby K. Operational conditions optimization of a proposed solar-powered adsorption cooling system: Experimental, modeling, and optimization algorithm techniques. *Energy*. 2020;206:118007. doi:10.1016/j.energy.2020.118007

7. Ali ES, Askalany AA, Harby K, Diab MR, Hussein BRM, Alsaman AS. Experimental adsorption water desalination system utilizing activated clay for low grade heat source applications. *Journal of Energy Storage*. 2021;43:103219. doi:10.1016/j.est.2021.103219

8. İnan AT, Köten H, Karta MA. Experimental comparison and CFD analysis of conventional shell and tube heat exchanger with new design geometry at different baffle intervals. *An International Journal of Computation and Methodology*. 2023;83:522-533.

9. İnan AT, Köten H, Kartal MA. CFD analysis and comparison of conventional type and perforated plate type shell tube heat exchangers. *International Journal of Low-Carbon Technologies*. 2022;17:1280-1291. doi:10.1093/ijlct/ctac033

10. Tso CY, Chao CYH, Fu SC. Performance analysis of a waste heat driven activated carbon based composite adsorbent – Water adsorption chiller using simulation model. *International Journal of Heat and Mass Transfer*. 2012;55(25-26):7596-7610. doi:10.1016/j.ijheatmasstransfer.2012.07.064

11. Miles DJ, Shelton SV. Design and testing of a solid-sorption heat-pump system. *Applied Thermal Engineering*. 1996;16(5):389-394. doi:10.1016/1359-4311(95)00021-6

12. Critoph RE. Performance estimation of convective thermal wave adsorption cycles. *Applied Thermal Engineering*. 1996;16(5):429-437. doi:10.1016/1359-4311(95)00026-7

13. Saha BB, El-Sharkawy II, Chakraborty A, Koyama S. Study on an activated carbon fiber-ethanol adsorption chiller: Part I- system description and modelling. *Int J Refrig*. 2007;30:86-95.

14. Saha BB, El-Sharkawy II, Chakraborty A, Koyama S. Study on an activated carbon fiber-ethanol adsorption chiller: Part II - performance evaluation. *Int J Refrig*. 2007;30:96-102.

15. Sadeghlu A, Yari M, Mahmoudi SMS, Dizaji HB. Performance evaluation of Zeolite 13X/CaCl2 two-bed adsorption refrigeration system. *International Journal of Thermal Sciences*. 2014;80:76-82. doi:10.1016/j.ijthermalsci.2014.02.001

16. Habiba K, Sahab BB, Chakrabortyc A, Koyamad S, Srinivasane K. Performance evaluation of combined adsorption refrigeration cycles. *Int J Refrig*. 2011;34:129-137.

17. El-sharkawy MM, Askalany AA, Harby K, Ahmed MS. Adsorption isotherms and kinetics of a mixture of Pentafluoroethane, 1,1,1,2-Tetrafluoroethane and Difluoromethane (HFC-407C) onto granular activated carbon. *Applied Thermal Engineering*. 2016;93:988-994. doi:10.1016/j.applthermaleng.2015.10.077

18. Ghazy M, Harby K, Askalany AA, Saha BB. Adsorption isotherms and kinetics of activated carbon/difluoroethane adsorption pair: theory and experiments. *Int J Refrig*. 2016;70:196-205. doi:10.1016/j.ijrefrig.2016.01.012

19. El-Sharkawy II, Hassan M, Saha BB, Koyama S, Nasr MM. Study on adsorption of methanol onto carbon based adsorbents. *Int J Refrig*. 2009;32(7):1579-1586. doi:10.1016/j.ijrefrig.2009.06.011

20. El-Sharkawy II, Kuwahara K, Saha BB, Koyama S, Ng KC. Experimental investigation on adsorption of ethanol onto activated carbon fibers for possible application in adsorption cooling system. *Applied Thermal Engineering*. 2006;26(8-9):859-865. doi:10.1016/j.applthermaleng.2005.10.010

21. Salehi E, Taghikhani V, Ghotbi C, Nemati Lay E, Shojaei A. Theoretical and Experimental Study on the Adsorption and Desorption of Methane by Granular Activated Carbon at 25°C. *Journal of Natural Gas Chemistry*. 2007;16(4):415-422. doi:10.1016/s1003-9953(08)60014-6

22. Al-Ghoutia MA, Yousef I, Ahmad R, Ghraira AM, Al-Maaitah AA. Characterization of diethyl ether adsorption on activated carbon using a novel adsorption refrigerator. *Chem Eng J*. 2010;162:234-241.

23. Wang RZ, Oliveira RG. Adsorption refrigeration—an efficient way to make good use of waste heat and solar energy☆. *Prog Energy Combust Sci*. 2006;32(4):424-458. doi:10.1016/j.pecs.2006.01.002

24. Theodore L. *Air Pollution Control Equipment Calculations*. John Wiley & Sons; 2008.

25. Perry RH, Green DW. *Perry's Chemical Engineers' Handbook*. 7th ed. McGraw-Hill; 1997.

26. Seader JD, Henley EJ. *Separation Process Principles*. New York, NY, USA; 1998.

27. Ullah KR, Saidur R, Ping HW, Akikur RK, Shuvo NH. A review of solar thermal refrigeration and cooling methods. *Renewable and Sustainable Energy Reviews*. 2013;24:499-513. doi:10.1016/j.rser.2013.03.024

28. Wang LW, Wang RZ, Oliveira RG. A review on adsorption working pairs for refrigeration. *Renewable and Sustainable Energy Reviews*. 2009;13(3):518-534. doi:10.1016/j.rser.2007.12.002

29. Meunier F, Douss N. Performance of adsorption heat pumps: active-carbon-methanol and zeolite-water pairs. In: *Trans. ASHRAE Meeting*. Saint Louis, USA; 1990:491-498.

30. Cacciola G, Restuccia G. Adsorption heat pumps: a new way for energy saving and CFCs replacement. Adsorption and its Applications in Industry and Environmental protection Studies. In: *Studies in Surface Science and Catalysis*. Vol 120. National Council of Research, Institute for Research on Chemical Methods and Processes for Energy Storage and Transformation; 1998:949-978. doi:10.1016/s0167-2991(99)80386-3

31. Yao L, Yage W, Bingqing C, Lanyun W, Juan Y, Binbin W. Integration and optimization of methanol-reforming proton exchange membrane fuel cell system for distributed generation with combined cooling, heating and power. *Journal of Environmental Chemical Engineering*. 2022;10:108847.

32. Mai B, Nabeel A, Yousef A. Modelling and performance assessment of a Tri–Generation cooling system using two adsorption chillers under Jordanian climate. *Case Studies in Thermal Engineering*. 2023;44:102848.

33. Jingkang L, Wenkui Z, Yunfeng W, Xu J, Ming L. Effect of cooling temperature on the performance of a solar adsorption chiller with the enhanced mass transfer. *Applied Thermal Engineering*. 2023;219:119611.

34. Anyanwu EE, Ezekwe CI. Design, construction and test run of a solid adsorption solar refrigerator using activated carbon/methanol, as adsorbent/adsorbate pair. *Energy Conversion and Management*. 2003;44(18):2879-2892. doi:10.1016/s0196-8904(03)00072-4

35. Wang LW, Wu JY, Wang RZ, Xu YX, Wang SG. Experimental study of a solidified activated carbon-methanol adsorption ice maker. *Applied Thermal Engineering*. 2003;23(12):1453-1462. doi:10.1016/s1359-4311(03)00103-0

36. Boubakri A, Guilleminot JJ, Meunier F. Adsorptive solar powered ice maker: experiments and model. *Solar Energy*. 2000;69(3):249-263. doi:10.1016/s0038-092x(00)00063-3

37. Leite APF, Daguenet M. Performance of a new solid adsorption ice maker with solar energy regeneration. *Energy Conversion and Management*. 2000;41(15):1625-1647. doi:10.1016/s0196-8904(00)00011-x

38. Li ZF, Sumathy K. A solar-powered ice-maker with the solid adsorption pair of activated carbon and methanol. *Int J Energy Res*. 1999;23(6):517-527. doi:10.1002/(sici)1099-114x(199905)23:6

39. Headley OS, Kothdiwala AF, Mcdoom IA. Charcoal-methanol adsorption refrigerator powered by a compound parabolic concentrating solar collector. *Solar Energy*. 1994;53(2):191-197. doi:10.1016/0038-092x(94)90481-2

40. Douss N, Meunier F. Effect of operating temperatures on the coefficient of performance of active carbon-methanol systems. *Heat Recovery Systems and CHP*. 1988;8(5):383-392. doi:10.1016/0890-4332(88)90042-7

41. Pons M, Guilleminot JJ. Design of an experimental solar-powered, solid-adsorption ice maker. *Journal of Solar Energy Engineering*. 1986;108(4):332-337. doi:10.1115/1.3268115

42. Saha BB, Chakraborty A, Koyama S, et al. Isotherms and thermodynamics for the adsorption of n-butane on pitch based activated carbon. *Int J Heat Mass Transf*. 2008;51(7-8):1582-1589. doi:10.1016/j.ijheatmasstransfer.2007.07.031

43. Habib K, Saha BB, Rahman KA, Chakraborty A, Koyama S, Ng KC. Experimental study on adsorption kinetics of activated carbon/R134a and activated carbon/R507A pairs. *Int J Refrig*. 2010;33(4):706-713. doi:10.1016/j.ijrefrig.2010.01.006

44. Hassan M. *Development of Thermally Powered Adsorption Refrigeration System*. Ph.D., Thesis. Thesis; 2013.

45. Saha BB, Boelman E, Kashiwagi T. Computer simulation of a silica gel-water adsorption refrigeration cycle-the influence of operating conditions on cooling output and COP. *ASHRAE Transactions*. 1995;101:348-357.